

Anomalous Increase of Dielectric Permittivity in Sr-Doped CCTO Ceramics $\text{Ca}_{1-x}\text{Sr}_x\text{Cu}_3\text{Ti}_4\text{O}_{12}$ ($0 \leq x \leq 0.2$)

Rainer Schmidt^{*,†,‡} and Derek C. Sinclair[‡]

[†]Universidad Complutense de Madrid, Departamento Física Aplicada III, GFMC, Facultad de Ciencias Físicas, Madrid 28040, Spain and [‡]The University of Sheffield, Engineering Materials, Sir Robert Hadfield Building, Mappin Street, Sheffield S1 3JD, United Kingdom

Received October 19, 2009

$\text{CaCu}_3\text{Ti}_4\text{O}_{12}$ (CCTO) is an 1:3 A-site ordered perovskite ($A'A''_3B_4O_{12}$), which has attracted a great deal of interest recently¹ due to exceptionally high dielectric permittivity values of up to $\sim 300\,000$ in polycrystalline ceramics,² ~ 700 in thin films,³ and $\sim 100\,000$ in single crystals.⁴ It has now been established that the origin of such high permittivity values is of extrinsic nature. It has been proposed that an internal barrier layer capacitor (IBLC) structure of conducting grains and insulating grain boundaries (GBs) is responsible for the high effective permittivity in polycrystalline ceramics.⁵ On the other hand, a surface barrier layer capacitor (SBLC) structure or electrode interface effects have been proposed to account for high effective permittivity in thin films and single crystals.³ Alternatively, the presence of domain boundaries in CCTO crystals have been claimed to be responsible for the high permittivity⁶ but such propositions have turned out to be controversial.⁷

Much effort has been dedicated to understand the origin of the extrinsic giant relative permittivity but little effort has been made to study the intrinsic (bulk) relative

permittivity, ϵ_r , which is in the range of ~ 100 .⁸ Although this is considerably smaller than the giant extrinsic values, it is still higher than would be expected in a nonferroelectric material from the polarizabilities of the constituent atoms. An additional mechanism, therefore, must be present to explain the high intrinsic ϵ_r of CCTO. In a recent study, $A'-A''$ antisite defects have been proposed to be responsible for such an increase in ϵ_r .⁹ Quantitative electron diffraction (QED) and extended X-ray absorption fine structure (EXAFS) analysis were employed to demonstrate Ca and Cu disorder in CCTO on a nanometric scale, and the increased ϵ_r was proposed to be a result of the modified electronic structure of the defect Cu cation on the A' site. We show here that partial substitution of Ca with Sr on the A' sites can lead to an anomalous increase in ϵ_r . Given the similar valence electron configuration of Ca and Sr, we argue that electronic structure variations are an unlikely origin of such ϵ_r increase and an alternative mechanism exists in $\text{Ca}_{1-x}\text{Sr}_x\text{Cu}_3\text{Ti}_4\text{O}_{12}$ (CSCTO).

$\text{Ca}_{1-x}\text{Sr}_x\text{Cu}_3\text{Ti}_4\text{O}_{12}$ ($0 \leq x \leq 0.4$) powders were synthesized from reagents of CaCO_3 (Aldrich, 99.995% purity), SrCO_3 (Alfa Aesar, 99.99%), CuO (Aldrich, 99.99%), and TiO_2 (Sigma-Aldrich, 99.99%). Mixing and grinding was performed using an agate pestle and mortar. At least 5 repeated mixing/grinding and synthesis cycles were required to fully react and homogenize each composition. In general, synthesis was performed at 950 °C in a Lenton muffle furnace for 8 and 12 h in successive cycles. For $x = 0$, heating at 1000 °C was required to achieve phase purity, as determined from X-ray diffraction (XRD) phase analysis. A high-resolution STOE STADI-P diffractometer (STOE & Cie GmbH, Darmstadt) with an image plate detector, $\text{Cu K}\alpha_1$ radiation in transmission mode, operated at 40 kV and 40 mA, was used. Pellets were pressed with a uniaxial hydraulic press (1 ton), and the green bodies sintered at 1000 °C for 12 h. To avoid the formation of SrTiO_3 secondary phase, the maximum sintering temperature was restricted to 1000 °C (see Supporting Information, Part I, for more details regarding the presence of SrTiO_3 in these samples). Scanning electron microscopy (SEM) using a JEOL microscope operating in backscattered electron mode was performed on polished pellets to confirm there was no SrTiO_3 present for each composition (Supporting Information, Part I). For lattice parameter determination we employed XRD with an internal Si standard using the STOE STADI-P diffractometer with a position sensitive detector (PSD).

A small amount of single-phase powder was heated at 1000 °C for 12 h to obtain the lattice parameter of the sintered pellets. The lattice parameter a of

*Corresponding author. E-mail: rainerxschmidt@googlemail.com.

- (1) (a) Ramirez, A. P.; Subramanian, M. A.; Gardel, M.; Blumberg, G.; Li, D.; Vogt, T.; Shapiro, S. M. *Solid State Commun.* **2000**, *115* (5), 217. (b) Homes, C. C.; Vogt, T.; Shapiro, S. M.; Wakimoto, S.; Ramirez, A. P. *Science* **2001**, *293*, 673. (c) Chung, S.-Y.; Kim, I.-D.; Kang, S.-J. L. *Nat. Mater.* **2004**, *3*, 774–778. (d) Sinclair, D. C.; Adams, T. B.; Morrison, F. D.; West, A. R. *Appl. Phys. Lett.* **2002**, *80*, 2153.
- (2) (a) Adams, T. B.; Sinclair, D. C.; West, A. R. *Adv. Mater.* **2002**, *14*, 1321. (b) Liu, J.; Smith, R. W.; Mei, W.-N. *Chem. Mater.* **2007**, *19*, 6020.
- (3) (a) Deng, G.; Yamada, T.; Muralt, P. *Appl. Phys. Lett.* **2007**, *91*, 202903. (b) Fiorenza, P.; Lo Nigro, R.; Sciuto, A.; Delugas, R.; Raineri, V.; Toro, R. G.; Catalano, M. R.; Malandrino, G. *J. Appl. Phys.* **2009**, *105*, 061634. (c) Si, W.; Cruz, E. M.; Johnson, P. D.; Barnes, P. W.; Woodward, P.; Ramirez, A. P. *Appl. Phys. Lett.* **2007**, *81*, 2056. (d) Deng, G. C.; He, Z. B.; Muralt, P. *J. Appl. Phys.* **2009**, *105*, 084106.
- (4) Kant, C.; Rudolf, T.; Mayr, F.; Krohns, S.; Lunkenheimer, P.; Ebbinghaus, S. G.; Loidl, A. *Phys. Rev. B* **2008**, *77*, 045131.
- (5) West, A. R.; Adams, T. B.; Morrison, F. D.; Sinclair, D. C. *J. Eur. Ceram. Soc.* **2004**, *24*, 1439. (b) Li, M.; Feteira, A.; Sinclair, D. C.; West, A. R. *Appl. Phys. Lett.* **2006**, *88*, 232903.
- (6) Subramanian, M. A.; Sleight, A. W. *Solid State Sci.* **2002**, *4*, 347. (b) Fang, T.-T.; Mei, L.-T. *J. Am. Ceram. Soc.* **2007**, *90*, 638.
- (7) Wu, L.; Zhu, Y.; Park, S.; Shapiro, S.; Shirane, G.; Taftø, J. *Phys. Rev. B* **2005**, *71*, 014118.

- (8) Lunkenheimer, P.; Fichtl, R.; Ebbinghaus, S. G.; Loidl, A. *Phys. Rev. B* **2004**, *70*, 172102.
- (9) Zhu, Y.; Zheng, J. C.; Wu, L.; Frenkel, A. I.; Hanson, J.; Northrup, P.; Ku, W. *Phys. Rev. Lett.* **2007**, *99*, 037602.

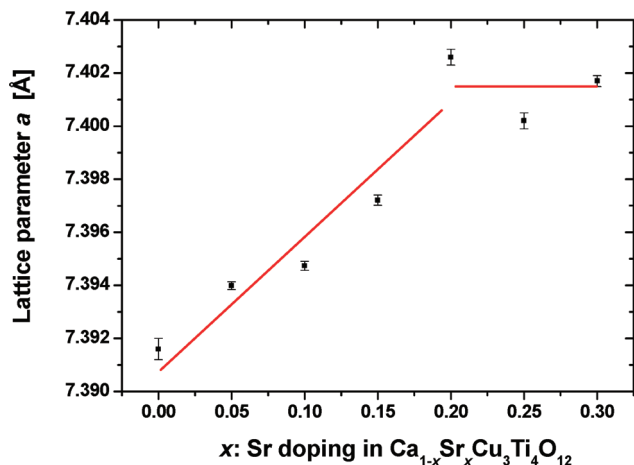


Figure 1. a versus x for $\text{Ca}_{1-x}\text{Sr}_x\text{Cu}_3\text{Ti}_4\text{O}_{12}$ fired at 1000 °C. Red lines are a guide for the eyes.

$\text{Ca}_{1-x}\text{Sr}_x\text{Cu}_3\text{Ti}_4\text{O}_{12}$ is shown in Figure 1. a increases for $0 \leq x \leq 0.2$ with increasing Sr-content and this is attributed to the larger cationic size of Sr (1.44 Å) compared to Ca (1.35 Å).¹⁰ For $x > 0.2$, no further increase of a was observed and we interpret this as the solid solution limit for this series. The formation of SrTiO_3 secondary phase was evident in the XRD patterns only for $x = 0.4$ (Supporting Information, Part I), which is consistent with the XRD resolution limit and the amount of SrTiO_3 expected.

In a recent publication, it has been shown that a Ca-free composition can be prepared,¹¹ however, this requires Sr-deficiency on the A' -site: $\text{Sr}_{0.946}(\text{Cu}_{2.946}\text{Ti}_{0.054})\text{Ti}_4\text{O}_{12}$ (SCTO). The lattice parameter of this nonstoichiometric phase was reported to be 7.43 Å,¹¹ which is slightly smaller than an estimate of 7.44 Å obtained by extrapolating data from our stoichiometric $0 \leq x \leq 0.2$ samples to $x = 1$. This small discrepancy may be consistent with the observed A' site Sr vacancies in SCTO.

For dielectric characterization, the 1000 °C sintered pellets were covered on both sides with Au electrodes using dc sputtering. Impedance spectroscopy (IS) was carried out at 10 and 100 K between 10 Hz and 2 MHz on $0 \leq x \leq 0.2$ single-phase samples within the solid-solution limit. An Agilent E4980A LCR meter and an Oxford Instruments closed-cycle He refrigerator were used to obtain the data. The real and imaginary parts of the complex impedance (Z' – Z'') were measured and converted into the complex capacitance formalism (C' – C'') using the standard conversion. Figure 2 shows plots of the real part of capacitance C' vs frequency (f) at 100 (a) and 10 K (b) for various x . The well-known dielectric heterogeneity of CCTO ceramics is preserved in Sr-doped samples, as is shown by the appearance of two distinct capacitance plateaus in Figure 2a. The low-frequency and high-capacitance plateau originates from the GB relaxation, whereas the high-frequency and low-capacitance plateau represents the intrinsic bulk permittivity.² The GB

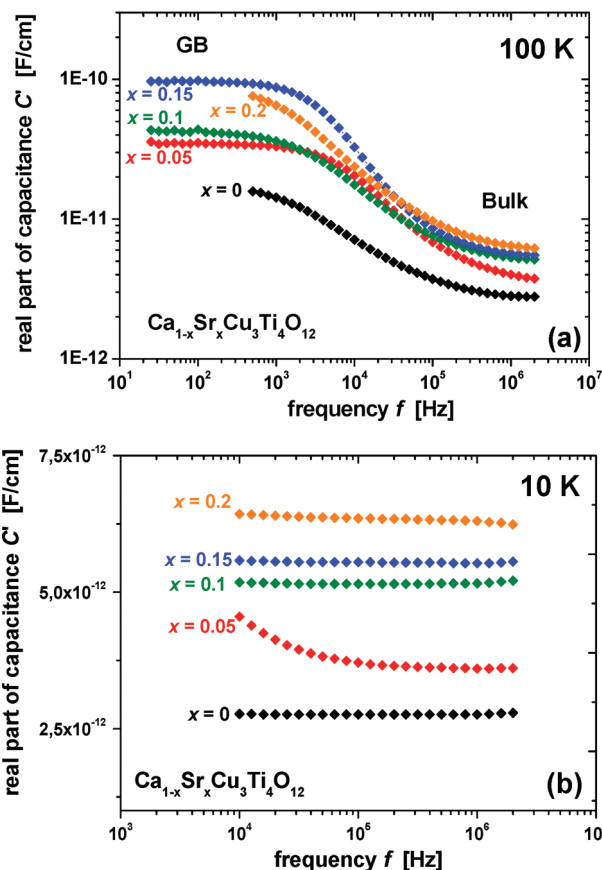


Figure 2. Real part of the capacitance C' normalized to the pellet geometry versus frequency f at (a) 100 and (b) 10 K.

capacitance is relatively small when compared to the giant extrinsic values reported previously. We associate this with the lower sintering temperature of the Sr-doped CCTO ceramics (1000 °C), where the IBLC structure is not fully developed. The IS data at 10 K do not display the GB relaxation (Figure 2b). The bulk capacitance dominates, and the low-capacitance plateau value can be regarded an estimate for the bulk capacitance. It has to be noted that the GB capacitance may influence the value of the high-frequency bulk capacitance plateau, and a correction of bulk capacitance values for this effect is necessary. Details of the correction procedure are given in Supporting Information, Part II.

Figure 2b demonstrates an increase in the uncorrected bulk capacitance with increasing Sr content x , which is preserved for corrected values (Figure 3). The capacitance at 1 MHz was determined, converted to relative dielectric permittivity values (ϵ_r), which were then corrected for the GB capacitance. Additionally, ϵ_r was corrected for the pellet density of each sample. Low pellet density ($\sim 80\%$ of the theoretical X-ray density) was a consequence of the restricted sintering temperature of 1000 °C required to avoid the formation of SrTiO_3 as a secondary phase. The correction for pellet density was carried out using Heidinger's approach.¹² These corrected values of ϵ_r are

(10) Shannon, R. D.; Prewitt, C. T. *Acta Crystallogr., Sect. B* **1969**, *25*, 925.

(11) Li, J.; Subramanian, M. A.; Rosenfeld, H. D.; Jones, C. Y.; Toby, B. H.; Sleight, A. W. *Chem. Mater.* **2004**, *16*, 5223.

(12) (a) Heidinger, R.; Nazare, S. *Powder Metall. Int.* **1988**, *20*, 30. (b) Penn, S. J.; Alford, N. M.; Templeton, A.; Wang, X.; Xu, M.; Reece, M.; Schrapel, K. *J. Am. Ceram. Soc.* **1997**, *80*, 1885.

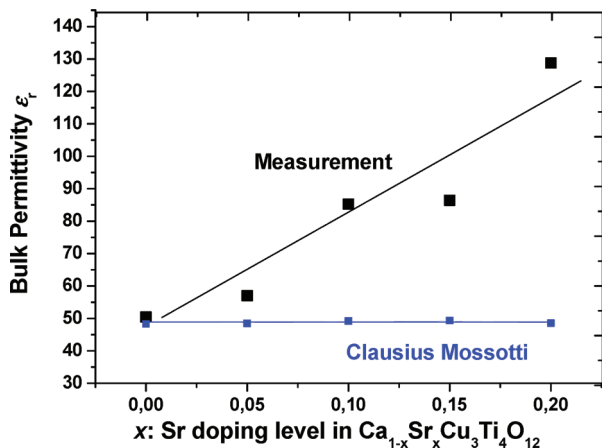


Figure 3. Fixed-frequency (1 MHz) intrinsic relative dielectric permittivity ϵ_r values (black squares) from the bulk relaxation process (measurement) at 10 K. Estimates of ϵ_r (blue squares) were calculated from the Clausius–Mossotti equation.

plotted vs x in Figure 3 (measurement). For comparison, ϵ_r for each x was also calculated using the Clausius–Mossotti (C–M) equation. The atom polarizabilities were obtained from Shannon,¹³ and the unit-cell volume was estimated for each composition using the lattice parameter values in Figure 1. It is noteworthy that the C–M calculations show no significant variation of ϵ_r with x . The measured increase in ϵ_r with x in Figure 3 cannot therefore be explained simply by the polarizabilities of the constituent atoms and changes in unit-cell volume. This anomalous increase of intrinsic bulk ϵ_r with x was confirmed from modulus M'' vs frequency data. (Supporting Information, Part II).

In the literature, several mechanisms have been proposed to explain high dielectric permittivity above the predictions from the atom polarizabilities according to the Clausius–Mossotti equation. In the particular case of CCTO, three possible explanations have been suggested: (1) A displacive ionic polarization in the unit cell leading to incipient ferroelectricity has been proposed.¹⁴ This is supported by reports of a phonon mode softening in CCTO.⁴ (2) A locally increased dielectric permittivity has been claimed to exist near the A' site Cu antisite defects exhibiting a local “metallic” dielectric response. Such local metallicity may arise because of the different electronic structure and crystal field splitting of the d-electron levels in defect Cu cations sitting on Ca sites.⁹ (3) A charge-transfer mechanism has been suggested to account for increased dielectric permittivity. This may occur if the chemical bonding changes to a more ionic type, leading to an effective electron transfer to the oxygen anions. The increased ionic character of the

bonding then leads to an increased contribution of ionic polarizability to the dielectric permittivity.^{4,15}

In our study, we can quite safely rule out mechanism 2, because Sr and Ca exhibit similar valence electron configurations. Mechanism 3 also seems unlikely, because the Pauling electronegativity of Sr (0.95) is reduced by only 5% when compared to Ca (1.00), and both values are small when compared to oxygen (3.44). In both cases, for Sr and Ca, strong ionic character of the bonding is expected. An increasing amount of Sr residing on the Ca sites in $\text{Ca}_{1-x}\text{Sr}_x\text{Cu}_3\text{Ti}_4\text{O}_{12}$ may therefore not account for the ~300% increase of ϵ_r from $x = 0$ to 0.2. Thus, we favor mechanism 1. A displacive ionic polarizability may come about because of the occurrence of local lattice stretches near Sr A' sites. The locally stretched lattice may result in a “rattling” of some of the neighboring ions, whereby the large Sr cation itself may not be the main candidate. Such a type of polarizability has been mentioned before in the literature to account for high dielectric permittivity above Clausius–Mossotti predictions.¹³ The proposed lattice stretches would be consistent with the Sr-deficiency in SCTO; at large Sr content, Ti occupancy of the square planar A'' site seems to be favorable over a full stoichiometric Sr occupation of the A' site for steric reasons because of the larger cationic size of Sr. Lattice stretches must therefore exist, and they exceed the tolerable extent within the CSCTO structure at high Sr-content leading to Sr vacancies.

We conclude that A' site Ca substitution by Sr can account for an anomalous increase in dielectric permittivity beyond the atomic polarizabilities and unit-cell volume of CSCTO ceramics. Because the valence electron configuration of Sr and Ca cations are similar, the reason for the increased ϵ_r in CSCTO may not be due to electronic structure variations. We propose that an alternative mechanism, possibly a locally stretched lattice near Sr A' sites and the resulting ionic displacements, may be regarded as the origin of the high intrinsic bulk dielectric permittivity. A similar scenario may also be applicable to undoped CCTO. Lattice stretches near defect A'' site Cu, or more likely near defect A'' site Ca, in CCTO may be an alternative explanation for the large bulk dielectric permittivity ϵ_r .

Acknowledgment. We thank the EU (NUOTO project) for financial support and Nik Reeves-McLaren, Andrew Mould, Peter Korgul and Heath Bagshaw for technical support.

Supporting Information Available: Phase analysis by XRD and SEM of $x = 0.2$ and 0.4 samples; impedance spectroscopy data analysis (PDF). This material is available free of charge via the Internet at <http://pubs.acs.org>

(13) Shannon, R. D. *J. Appl. Phys.* **1993**, *73*, 348.

(14) Ferrarelli, M. C.; Sinclair, D. C.; West, A. R.; Dabkowska, H. A.; Dabkowski, A.; Luke, G. M. *J. Mater. Chem.* **2009**, *19*, 5919.

(15) Homes, C. C.; Vogt, T.; Shapiro, S. M.; Wakimoto, S.; Subramanian, M. A.; Ramirez, A. P. *Phys. Rev. B* **2003**, *67*, 092106.